ELECTRIC POWER
RESEARCH INSTITUTE

Steam Generator Management Program: Model Assisted Probability of Detection of Eddy Current Steam Generator Inspection Indications

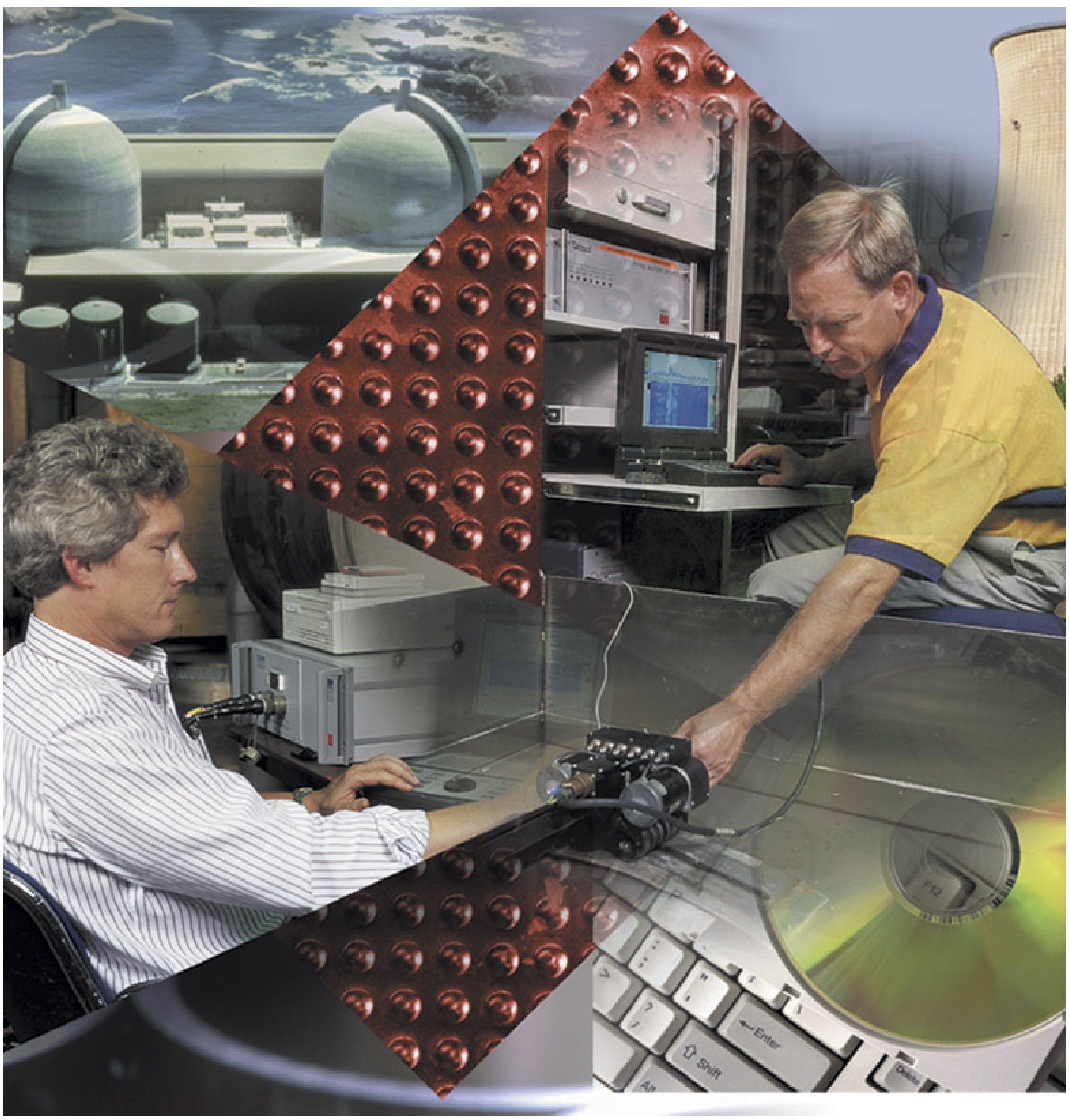

PORTIONS
TRANSLATED

Steam Generator Management Program: Model Assisted Probability of Detection of Eddy Current SG Inspection Indications

1020630

Technical Update, March 2010

EPRI Project Manager

T. Bipes

Work to develop this product was completed under the EPRI Nuclear Quality Assurance Program in compliance with 10 CFR 50, Appendix B and 10 CFR Part 21,

YES NO

ELECTRIC POWER RESEARCH INSTITUTE
3420 Hillview Avenue, Palo Alto, California 94304-1338 ▪ PO Box 10412, Palo Alto, California 94303-0813 ▪ USA
800.313.3774 ▪ 650.855.2121 ▪ askepri@epri.com ▪ www.epri.com

DISCLAIMER OF WARRANTIES AND LIMITATION OF LIABILITIES

ORGANIZATION(S) THAT PREPARED THIS DOCUMENT

Michigan State University

This is an EPRI Technical Update report. A Technical Update report is intended as an informal report of continuing research, a meeting, or a topical study. It is not a final EPRI technical report.

NOTE

For further information about EPRI, call the EPRI Customer Assistance Center at 800.313.3774 or e-mail askepri@epri.com.

CITATIONS

This document was prepared by

Michigan State University
East Lansing, MI 48824

Principal Investigator
L. Udpa
X. Liu
L. Zhang

This document describes research sponsored by the Electric Power Research Institute (EPRI).

This publication is a corporate document that should be cited in the literature in the following manner:

Steam Generator Management Program: Model Assisted Probability of Detection of Eddy Current SG Inspection Indications. EPRI, Palo Alto, CA: 2010 1020630.

PRODUCT DESCRIPTION

In the inspection of aging aircrafts, power plants, and gas transmission pipelines, it is important to ascertain whether the inspection system actually meets the inspection requirements. In these applications, the capability of an inspection system to detect critical flaws is quantified in terms of its probability of detection (POD) and observed confidence bounds. Limitations of different nondestructive inspection techniques and inspector variability often lead to false rejections and false acceptance errors. Further, uncertainties in operational parameters such as lift-off, probe wobble (offset), coil tilt, material properties, and flaw orientation lead to a spread in signal strength for the same nominal flaw size. Quantitative knowledge of the signal spread caused by these variables and uncertainties in inspection parameters can help operators rationalize their decision strategy. The estimation of POD with a good confidence bound requires a significant amount of experimental data. Very often, the experimental data are collected under near ideal conditions, which can lead to false estimates of POD.

In this project, the simulation model developed through another project with a user interface is used to generate a database and to conduct a systematic model-based study for calculating POD of critical flaws in critical locations. Quantitative knowledge of uncertainties of experimental parameters can be used in conjunction with numerical models to generate POD curves. Quantitative assessments based on POD models can then be used to accurately evaluate the performance of an inspection system under appropriate conditions.

Results and Findings

In this report, a model-based approach for POD calculation for steam generator (SG) tube geometry is presented. The approach is first applied to perform a sensitivity analysis of the POD with respect to different sources of variability in the eddy current SG inspection process. An initial set of parameters representing the sources of uncertainty was identified with input from the Electric Power Research Institute (EPRI). The concept was demonstrated using a probe/coil offset parameter and its effect on the resultant POD. The approach can therefore be used to study the effect of a single source of uncertainty on the resultant signal and subsequently to optimize inspection setup and probe construction.

Challenges and Objectives

A variety of tube/defect geometries and inspection parameters can be simulated using the SGTSIM3D software and the POD curves for various tube and flaw geometries, such as freespan, tube support-center/edge, tubesheet, expansion transition-explosive/hardroll, anti-vibration bar (AVB), sludge pile, loose part, and U-bend, can be generated as well as defect types such as inside diameter (ID), outside diameter (OD), axial, circumferential, stress corrosion cracks (SCCs), dents, manufacturing buff marks (MBMs), wears, and pits. POD curves for various probe types—such as bobbin, pancake, +pt, and array probes—can also be generated.

Applications, Value, and Use

The effect of different sources of uncertainty on POD curves can be used in optimizing probe/system design and operation. An uncertainty factor with a dramatic effect on POD can be identified as a “sensitive” factor in the probe/system design.

EPRI Perspective

Physics-based computational models providing the solution to mathematical (integral or differential) equations that describe the underlying physics of an inspection process can play a significant role in the generation of POD curves. These models enable the visualization of field and current distributions in the inspected parts, which in turn helps to optimize inspection parameters and enhances the reliability of inspection procedures. Models have been used in several industries as the way to study and trend the effects of uncertainties on signal strength. After the statistical distribution of signal amplitude is established using numerical computations, the POD and false calls can be estimated by integrating the signal distribution within the acceptance range.

Approach

Researchers used computational modeling along with data from the field, such as noise distributions, to replicate experimental data through computer modeling. Results are obtained in much less time and with much less cost compared to experimental approaches.

Keywords

Probability of detection
Modeling
Steam generator

CONTENTS

LIST OF FIGURES

LIST OF TABLES

1
INTRODUCTION

1.1 Steam Generator Tube

A steam generator is a typical heat exchanger used in nuclear power plants, as shown in Figure 1-1. Steam generators (SG) transfer heat from the primary loop to the secondary loop feedwater circulating on the outside of the tubes to produce steam that drives the turbines.

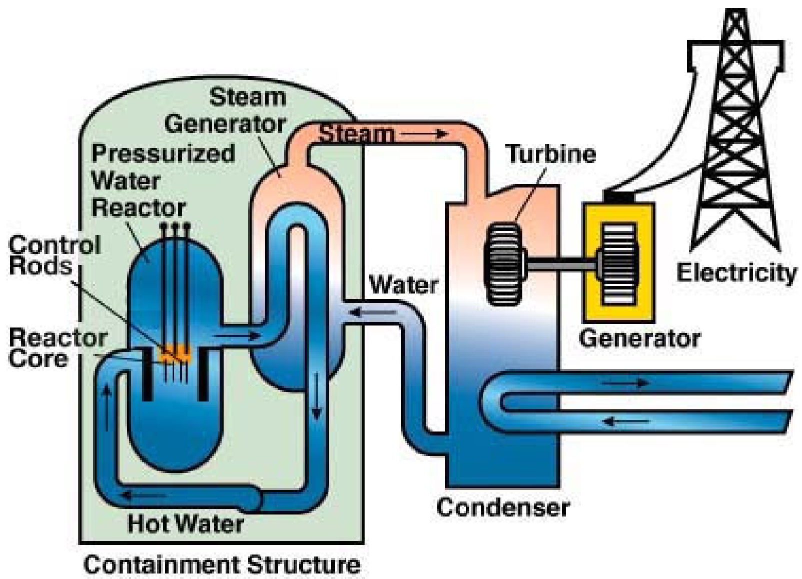

Figure 1-1
Steam Generator in Nuclear Power Plant

It is critical that the radioactive primary coolant does not leak into the secondary side. The steam generator tubes are continuously exposed to harsh environmental conditions including high temperatures, pressures, fluid flow rates and material interactions resulting in various types of degradation mechanisms such as mechanical wear between tube and tube support plates, outer diameter stress corrosion cracking (ODSCC), pitting, volumetric changes, primary water stress corrosion cracking (PWSCC), and inter granular attack (IGA). These flaws can result in tube thinning and/or development of multiple crack-like flaws, thereby increasing the risk for contaminating the fluids on the secondary side. Consequently the steam generator tubes in nuclear power plants are required to be inspected periodically for degradation.

Eddy current inspection has proven to be a fast and effective way to detect and size most degradation mechanisms that occur in steam generators. As the nation's generators have become older, more challenging forms of degradation have been observed that require more advanced application of eddy current testing.

1.2 Eddy Current Testing

The basic principle underlying such methods can be illustrated with a simple arrangement shown in Figure 1-2. When a coil carrying an alternating current is brought in close proximity to an electrically conducting test specimen, the alternating magnetic field causes induced currents in the conducting test specimen in accordance with Faraday's law of electromagnetic induction. The induced currents are called eddy currents since they follow closed circulatory patterns that are similar to eddies found in water bodies. The alternating eddy current, in turn, establishes a field whose direction is opposite to that of the original or primary field. Consequently, the net flux linkages associated with the coil decrease. Since the inductance of a coil is defined as the number of flux linkages per ampere, the effective inductance of the coil decreases relative to its value if it were to be suspended in air. The presence of eddy currents in the test specimen also results in a resistive power loss. The effect of this power loss manifests in the form of a small increase in the effective resistance of the coil. An exaggerated view of the changes in the terminal characteristics of the coil is shown in Figure 1-3, where the variation in resistance and inductance is plotted in the impedance plane. When a flaw or in-homogeneity whose conductivity and/or permeability differ from that of the host specimen is encountered, the current distribution is altered. Consequently, the impedance of the coil will be different relative to the value observed for unflawed regions. Systems that are capable of monitoring the changes in impedance can, therefore, be used to detect flaws in a specimen that is scanned by a coil.

Eddy currents exhibit a unique phenomenon known as the "skin effect" which causes the current density at a particular depth to decrease with an increase in the frequency of excitation. Skin depth (δ), also called standard depth of penetration, is defined as the depth at which eddy current density has decreased to 1/e of the surface value. The skin depth can be computed as follows:

$$\delta = \frac{1}{\sqrt{\pi \mu f \sigma}}$$

Equation 1-1

Where f is the excitation frequency of the circuit, μ is the magnetic permeability of the target material, and σ is the electrical conductivity of the target material. The skin depth is often used as a guideline to select the excitation frequency for testing a given specimen.

The variations in coil impedance caused by discontinuities in the test specimen are often very small in comparison with the quiescent value of the coil impedance. The detection and measurement of the small changes are often made possible with the use of bridge circuits.

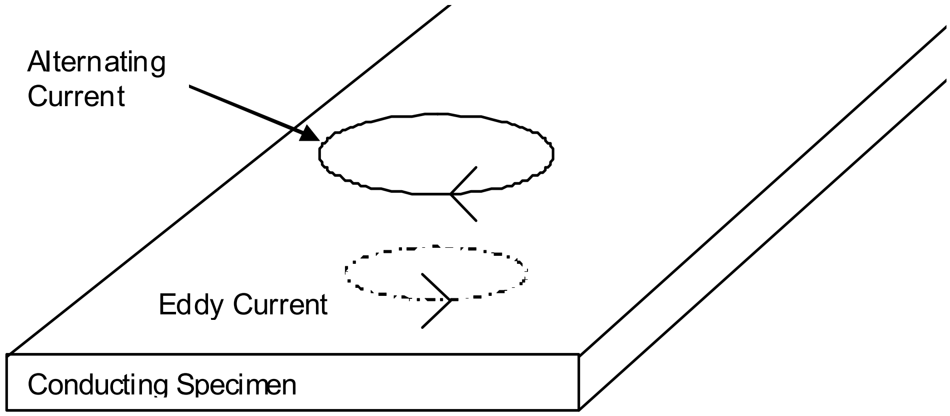

Figure 1-2
Eddy Current Generation and Flow in a Conducting Specimen

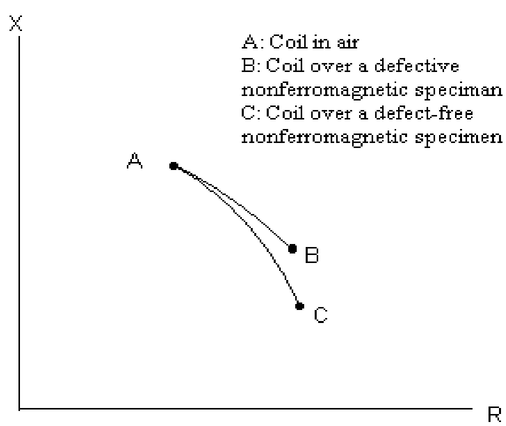

Figure 1-3
Impedance-Plane Trajectory of a Coil over a Conducting Test Specimen

Factors that influence the eddy current field, and therefore coil impedance are:

- Separation between the coil and specimen surface, called lift-off
- Electrical conductivity of the specimen
- Magnetic permeability of the specimen
- Frequency of the AC
- Design of the eddy current probe
- Specimen geometric factors
- Discontinuities, such as cracks, corrosion, pitting

Successful detection and characterization of flaws can benefit from a clear understanding of field/flaw interaction and effects of various probe signal operational parameters. Correlations between operational parameters and signal features help in signal processing design procedures to compensate for these effects and eliminate undesired responses. Correlations between defect parameters and signal features can help in designing more accurate detection and characterization algorithms. In particular, these correlations can be used to select features that maximize the Probability of Detection (POD) of defects in different locations of the steam generator.

1.3 Need for POD Study

In the inspection of aging aircrafts, power plants and gas transmission pipelines, it is important to ascertain that the inspection system actually meets the inspection requirements. In these applications, the capability of an inspection system to detect critical flaws is quantified in terms of its POD and observed confidence bounds. Limitations of different nondestructive inspection techniques and inspector variability often lead to false rejections and false acceptance errors. Further, uncertainties in operational parameters, such as lift-off, probe wobble (offset), coil tilt, material properties and flaw orientation lead to a spread in signal strength for the same nominal flaw size. Quantitative knowledge of the signal spread due to these variability and uncertainties in inspection parameters can help operators rationalize their decision strategy. **However, the estimation of POD with a good confidence bound requires a significant amount of experimental data. Very often, the experimental data is collected under near ideal conditions. These can lead to false estimates of POD.**

Physics based computational models providing the solution to mathematical (integral or differential) equations that describe the underlying physics of an inspection process can play a significant role in generating POD curves. These models enable the visualization of field and current distributions in the parts that are inspected, which in turn, helps in optimizing inspection parameters and enhances reliability of inspection procedures. Models have been used in several industries as the means by which effects of uncertainties on signal strength are studied and trended. Once the statistical distribution of signal amplitude is established using numerical computations, the probabilities of detection and false calls can be estimated by integrating the signal distribution within the acceptance range.

In this project the simulation model developed under EPRI contract with a user interface is used for database generation and conduct a systematic model based study for calculating POD of critical flaws in critical locations. Quantitative knowledge of uncertainties of experimental parameters can be used in conjunction with numerical model to generate POD curves. Quantitative assessments based on POD models can be used to accurately evaluate performance of an inspection system under appropriate conditions.

1.4 Review of Prior EPRI POD Work

Previous EPRI POD work is based on either empirical POD or MAPOD approach. Three of the reports generated were studied in this section, a brief summary of work conducted under the *Tools for Integrity* EPRI projects is presented.

Report 1 - Updates on the tools for integrity assessment project [1]

In this report, the multiple NDE analyst performance tests are conducted to obtain POD and NDE sizing uncertainty correlations. Ten analysis teams for detection and sizing testing were used, with the conclusion that 5 teams are sufficient for data sufficiency requirements.

Report 2 - Measuring and monitoring noise in steam generator tubing eddy-current data for tube integrity applications [2]

In this report, the methodologies to measure and monitor eddy current data for noise that could affect the performance indices are developed. Noise measurement consists of reporting noise amplitude data in each region of interest (ROI) and constructing noise amplitude cumulative distributions. Noise monitoring consists of reporting only those amplitudes which exceed a pre-established voltage threshold. **(It should be noted that the cumulative distributions of measurement noise are not Gaussian and zero mean as assumed in the MAPOD software in POD calculations).**

Report 3 - Tools for integrity assessment project technical report [3]

In this report, recommended examination scope for noise measurement and monitoring and implementation examples for baseline noise measurements, noise monitoring, and current outage noise measurements are provided. Software for measuring and monitoring noise are discussed.

All industry pulled tube data were gathered for ODSCC in the area of interest and procedures and protocols were used in a peer review to develop five data sets: three bobbin coil and two plus point (+pt) coil data sets. A performance demonstration was conducted, as well as POD and sizing. Summary of the tools for integrity program uncertainties were evaluated for the five data sets. The appendices of this report document the results of the pilot project.

1.5 Limitations of Prior Work

Traditional POD evaluation methodologies are entirely empirical. In this approach, flaw signals and their variability are determined using large number experimental measurements from samples. The experimental data are used to estimate the POD of the flaw. Unfortunately the determination of the POD requires a rather extensive set of measurements to obtain statistically sound estimates. In general, this approach for generating POD curves is time consuming and expensive. It involves the manufacturing of the defects in a large number of samples and requires a large number of operators, which may delay or prevent a new probe or new technology from being implemented.

The limitations of the empirical POD are overcome by Model assisted POD (MAPOD), incorporating numerical modeling and statistical approach to reduce the number of samples required. MAPOD is based on a logistic regression statistical model and has been successfully implemented in many NDE applications. Some of the limitations of MAPOD approach are listed below.

Primarily, there are the mandatory requirements for a valid regression model [4]. If the requirements are violated, the resulting regression model will be invalid and the conclusions based on it will necessarily be in error.

There are mandatory requirements for ordinary regression and all four must be satisfied:

1. Linearity of the parameters.
2. Uniform variance (homoscedasticity)
3. Conditionally uncorrelated observations
4. Normal distributed errors

The most often violated requirement is the normally distributed errors. In the model based POD (MBPOD) approach proposed in this report the above limitations are overcome by using Monte Carlo simulation procedure for estimating the probability density function (pdf) which is integrated to estimate the POD. Hence there are no requirements 1-4 in the proposed MBPOD approach.

1.6 Research Objectives

The objective of this project is to use the computational model developed in the EPRI sponsored Simulation Model project to initiate the studies necessary for calculating POD curves relevant for SG inspection.

These geometries include:

- Drilled support structures
- Top of tube-sheet (TTS)
- Free span
- Defect geometries (e.g., dents, dings, MBM’s, bulges, and foreign objects)

The probes include absolute and differential bobbin, pancake and +pt rotating probes.

The POD of critical flaws varies with location largely by virtue of different sources of uncertainties in each scenario. The objective of this project is to systematically identify the sources of uncertainties and generate a POD map of critical flaws in different locations.

2
MODEL BASED POD

2.1 Introduction

Reliability of nondestructive testing techniques is of considerable concern to the NDE community. In general, signals generated by identical flaws are usually different under practical testing conditions thereby affecting the accept/reject decision. Repeated inspections of a specific flaw can produce different magnitudes of response because of minute variations in setup and calibration. Different operators may make different decisions when analyzing the same signal.

POD models constitute a powerful tool for quantifying the reliability and assessing the applicability of a selected NDE technique. The POD model accounts for the variability that affects the output signal and generates a distribution of the signal around its mean value. This section describes a model based POD evaluation method, which is then used to optimize experiment setup.

2.2 Sources of Variability

The first step in computing probability of detection is to find out the sources of variability. Typical sources of variability of an NDE system include [5]

- Human factors
- Variations in specimen geometry, such as surface roughness and defect shape and dimensions
- Variations in excitation source such as current or voltage value
- Variations in material property, such as permeability, conductivity
- Variations in experimental parameters such as probe wobble (offset), gain, frequency
- Instrumentation/measurement noise

2.3 POD Concepts

The POD of a particular flaw of a given size using a given measurement system can be determined by generating conditional probability density functions (pdf) of the measurement signal. Figure 2-1 shows a typical conditional pdf of the peak signal value in the absence of a flaw, $p(y \mid x_0)$, and in the presence of a flaw, $p(y \mid x_1)$, where y is the peak value and x_0 and x_1 represent the “no-flaw” and “flaw” situations respectively.

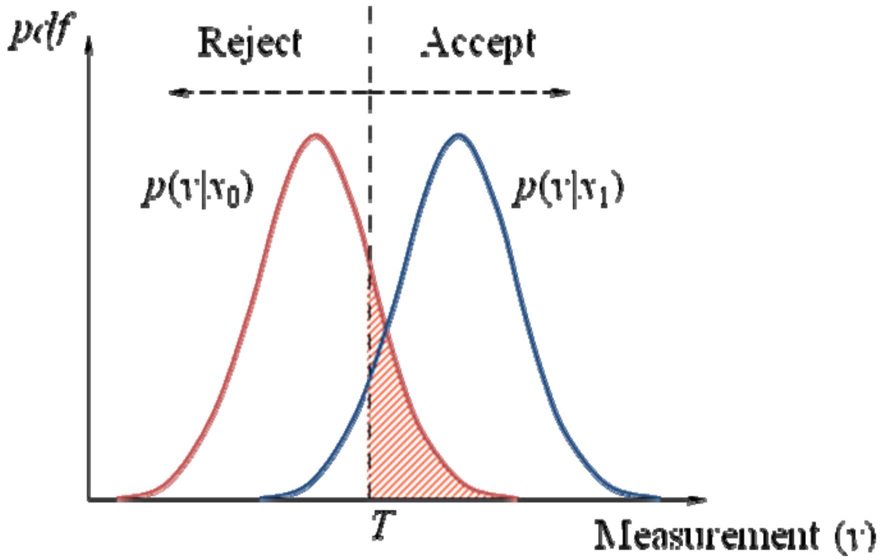

Figure 2-1
Typical Distributions of Flaw/no Flaw Signals

Choosing a threshold (T) as shown, all signals above the threshold is classified as flaw signals and signals below the threshold are interpreted as noise. Hence POD is determined by

$$POD = \int_{T}^{\infty} p(y \mid x_1) dy$$ **Equation 2-1**

If the pdf of flaw signal and noise overlap, as shown in Figure 2-1, the data interpretation based on threshold detection will involve two types of errors:

- Probability of False Alarm (PFA): The component without flaw is rejected due to incorrect interpretation of noise as a flaw indication and is determined by

$$PFA = \int_{T}^{\infty} p(y \mid x_0) dy$$ **Equation 2-2**

- Probability of False Acceptance (POFA): The component with flaw is accepted due to incorrect interpretation of a small flaw signal as noise fluctuations and is determined by

$$POFA = \int_{-\infty}^{T} p(y \mid x_1) dy$$ **Equation 2-3**

  POFA is related to POD by

$$POFA = 1 - POD$$ **Equation 2-4**

The Relative Operating Characteristic (ROC) shows the relationship between POD and PFA. Hence there is a trade-off between a high POD and a low PFA. Figure 2-2 shows a typical ROC curve.

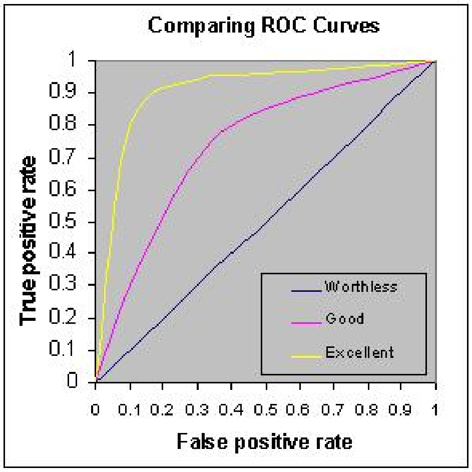

Figure 2-2
Typical ROC Curve

2.4 Selection of Thresholds

The threshold T can be selected using an appropriate criterion. Various criteria for selecting the threshold are:

1. Set PFA to a constant

In many practical applications it is desired to keep the PFA as low as possible. The PFA is independent of the pdf of the flaw signal and dependent only on the pdf of the background noise. The threshold is selected such that the PFA is a constant.

2. Set POD of the critical flaw size to a constant

This scheme is useful when the inspection system is expected to detect only flaws that are bigger than a critical size. The threshold is chosen such that the critical flaw is detected with a specified POD.

3. Minimization of the total signal classification error

In this scheme, the threshold is selected to minimize the sum of the overall error in signal classification, which is given by

$$E(T) = \int_{-\infty}^{T} p(y \mid x_1)dy + \int_{T}^{\infty} p(y \mid x_0)dy$$

Equation 2-5

where P is the prior probability of a flaw being present in the test specimen.

In this report, we using method based on the first method to select threshold. Threshold is selected so that POD of 10% defect = 0.75.

2.5 Model Based POD Approach

A schematic of the overall procedure for estimating the probability density functions is illustrated in Figure 2-3. A finite element model predicts the signals using the tube and defect geometry and values of selected variability parameter, such as probe offset. A family of curves are generated for increasing defect depths for each value of of probe offset. A family of regression models is generated using simple curve fitting procedure. These functions establish the relationship between signal magnitude vs. the selected variability parameter (probe offset) for each defect size. A Monte Carlo procedure then maps values of the variability parameter, with some distribution (input pdf), to generate the conditional prabability density functions of the signal magnitudes (output pdf's), $p(y \mid x_0)$ in the absence of flaw and $p(y \mid x_1)$ in the presence of a flaw, corresponding to the pdf of the perturbed parameter.

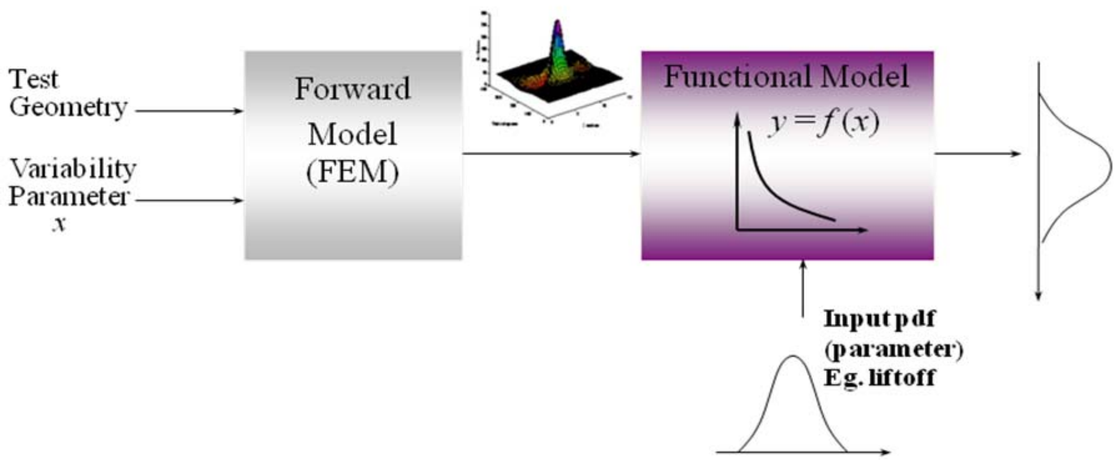

Figure 2-3
Procedure for Generating Conditional Probability Density Functions

Once the conditional pdf's are generated, the probability of detection can be evaluated using Equation 2-1 with appropriately selected threshold.

3
APPLICATION OF MODEL BASED POD

3.1 Introduction

The first step in POD calculation is to determine the sources of variablities, which affect the measured signal. In EPRI SG tube eddy current inspections, typical sources of variablities include: tube geometry, structure influence, foreign object influence, deposit influence, tube noise, probe construction (type and size), material variations, defect parameters, etc.

In Table 3-1, we list some of the variabilities considered.

Table 3-1
Uncertainties in SG Tube ECT

Data	Numerical model (SGTSIM3D)
Tube Geometry	freespan, tube support-center/edge, tube sheet, expansion transition, explosive/hardroll, AVB, sludge pile, loose part, U-Bend
Defects	ID-, OD-, axial-, circ-, SCCs, dents, MBMs, wears, pits
Probe	bobbin/ pancake/ +pt / array
Parameters	tube noise (use distributions generated by noise monitoring project), coil lift-off, probe wobble (offset), probe tile, frequency, tube material property (permeability, conductivity), sludge material, defect parameters (depth, length), loose part parameters and material properties

Besides the variabilities listed above there is also measurement noise which varies in different locations in the tube as described in the EPRI Report on *measuring and monitoring noise in steam generator tubing eddy-current data for tube integrity applications* [2]. Once the parameters are identified the range of the parametric variation is determined as listed in Table 3-2. The underlined value of the parameter is the default value used in steam generator tube inspection setup.

Table 3-2
Range of Parameters for Bobbin Probe

Parameters	Range of values for parameters
Defect orientation	ID/Ax, OD/Ax, ID/Circ, OD/Circ
Defect depth	0%, 20%, 40%, 60%, 80% and 100%
Defect length (inch)	0.15, 0.23, 0.3, 0.4, 0.5
Probe coil ID (inch)	0.46, 0.47, 0.48, 0.49, 0.50, 0.51, 0.52
Probe coil OD (inch)	0.57, 0.58, 0.59, 0.60, 0.61, 0.62, 0.63
Probe coil Height (inch)	0.057, 0.058, 0.059, 0.06, 0.061, 0.062, 0.063
Probe coil Spacing (inch)	0.057, 0.058, 0.059, 0.06, 0.061, 0.062, 0.063
Probe wobble/offset (inch)	-0.08, -0.06, -0.04, -0.02, 0, 0.02, 0.04, 0.06, 0.08
Probe tilting (degree)	-5, -4, -3, -2, -1, 0, 1, 2, 3, 4, 5
Operating frequency (kHz)	100, 150, 200, 250, 300, 350, 400, 450, 500
Conductivity of tube (S/m)	7.5e5, 8e5, 8.5e5, 9e5, 9.69e5, 10e5, 10.55e5, 11e5, 11.5e5
Tube dimension: inner diameter (inch)	0.700, 0.720, 0.740, 0.760, 0.775, 0.800, 0.820, 0.840, 0.860
Tube dimension: outer diameter (inch)	0.800, 0.820, 0.840, 0.860, 0.877, 0.900, 0.920, 0.940, 0.960

3.2 POD with respect to Offset of Bobbin Probe during a Scan

During scanning, the probe/coil should be set at the center of the tube (offset equal to zero). In Figure 3-1, we show the two-dimensional (2-D) cross section view of the tube, with a defect. Figure 3-1 (a) shows the case when the offset value is zero, Figure 3-1 (b) shows the case when the offset value is positive (probe closer to defect) and Figure 3-1 (c) shows the case when the offset value is negative (probe farther from defect).

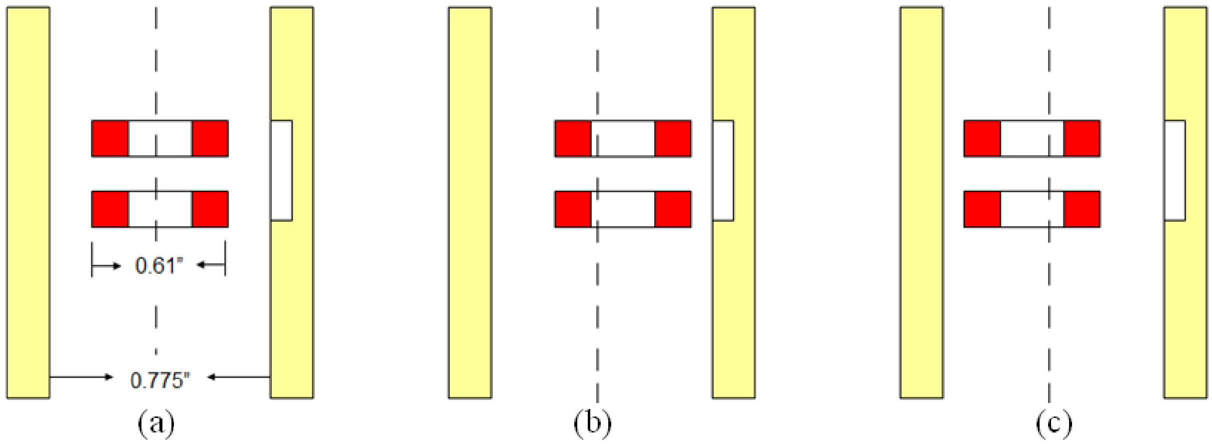

Figure 3-1
2-D Cross Section of Tube Geometry with Probe Offset (a) Zero Offset (b) Positive Offset (c) Negative Offset

SGTSIM software is used to predict signal for the given test geometry. The test geometry and model parameters are listed in Table 3-3. The defects are rectangular, ID axial defect. The length and width of the defect are 0.5” and 0.005”, respectively. The defect depths are 0 (defect-free), 20%, 40%, 60%, 80%, 100% (through-defect). The variability parameter is probe/coil offset ranging from -0.08” to 0.08”. The material of the tube is inconel 600, with permeability equal to 1.01 and conductivity equal to 969000. The probe is 0.610” HF bobbin coil. The operation frequency of the excitation current is 300 kHz. The impedance plane trajectory plots are generated and the signal features based on the trajectory plots are extracted for calculating the POD.

Table 3-3
Test Geometry

Geometry	Free Span
Defect	Rectangular, ID, axial, angle (90), depth (0, 20%, 40%, 60%, 80%, 100%), length (0.5”), width (0.005”)
Material	Tube (inconel 600 with permeability equal to 1.01 and conductivity equal to 969000)
Probe	0.610” HF bobbin coil
Operation frequency	300 k

For each defect depth, the signal is stronger, when the probe/coil is close to the defect (positive offset). For 0% defect, the measured signal is the random noise.

3.2.1 Selection of Signal Features

Features in the signal are used to generate the â vs. a curve. In this report, two different features are considered and evaluated using POD as measure for effectiveness. These are the maximum signal magnitude (Feature I) and magnitude of projected signal (Feature II) as explained in the following sections.

3.2.1.1 Maximum Signal Magnitude

Figure 3-2 illustrated the definition of maximum signal magnitude based on the trajectory plot of the bobbin probe signal. Feature I is plotted as a function of defect depth and different probe/coil offsets in Figure 3-3. A 3^{rd} order polynomial curve is fit to this data and serves a functional model of the â vs. a curves.

Assuming the probe/coil offset variations is distribution Gaussian, the corresponding conditional pdf’s of the signal magnitudes for defects of different depths are obtained using Monte Carlo simulation and the functional model. Since the functional models are non-linear (3^{rd} order polynomial functions), the conditional pdf’s of feature I are not necessarily Gaussian. The resulting conditional pdf curves are plotted in Figure 3-4.

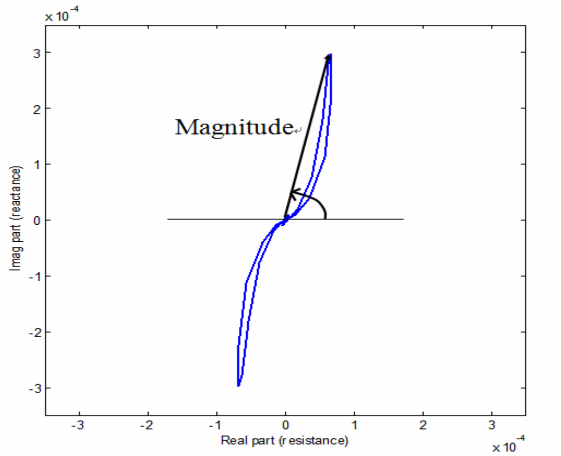

Figure 3-2
The Signal Magnitude Feature

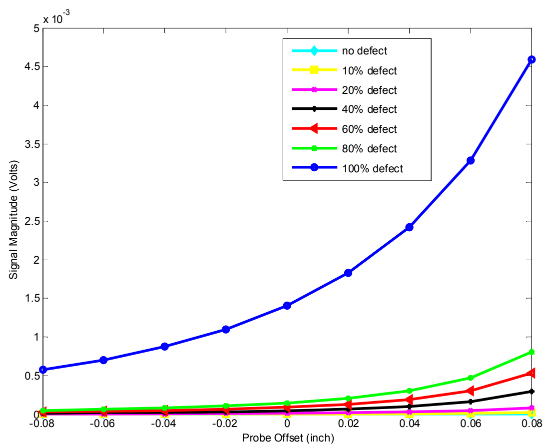

Figure 3-3
Signal Magnitude for Different Probe/Coil Offset

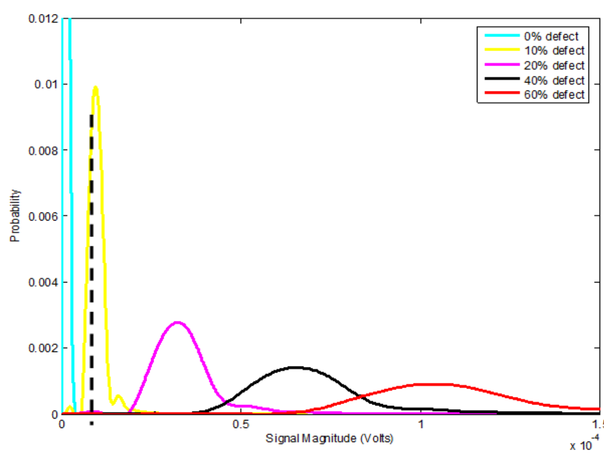

Figure 3-4
Pdf of Signal Magnitudes with 0%, 10%, 20%, 40%, and 60% Defect Depth

From Figure 3-4, the threshold is selected so that the POD of 10% defect is 75%. The cumulative PDF is obtained by integrating to the right of the threshold to estimate the POD of each defect. The POD curves for different probe offsets are similarly calculated and plotted in Figure 3-5.

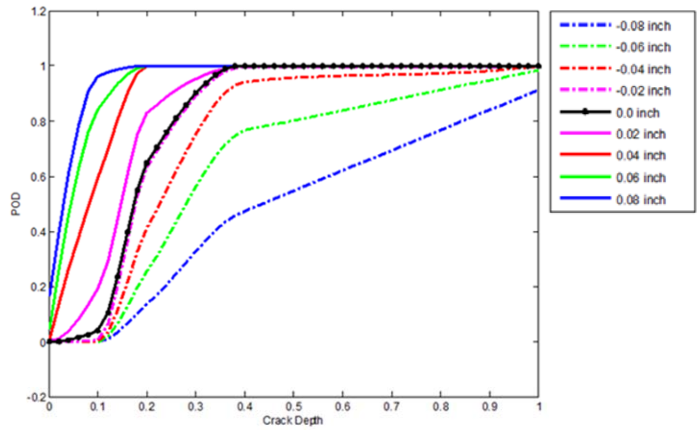

Figure 3-5
POD vs Defect Depth Curves for Different Probe Offsets

3.2.1.2 Magnitude of Projected Signal

The bobbin probe signal includes both real and imaginary parts. A projected signal which combines the two parts is calculated and used to compute feature II. Equation 3-1 describes the mathematical definition of the projected signal at angle α .

$$S_{project\_\alpha} = S_{real} \cdot \cos(\alpha) + S_{imag} \cdot \sin(\alpha)$$ **Equation 3-1**

Feature II is the maximum signal magnitude of the projected signal and is a function of the projection angle α. The signals at angles α_1 and α_2 are plotted in Figure 3-6. An optimum projection angle (OPA) can be selected to maximize the POD.

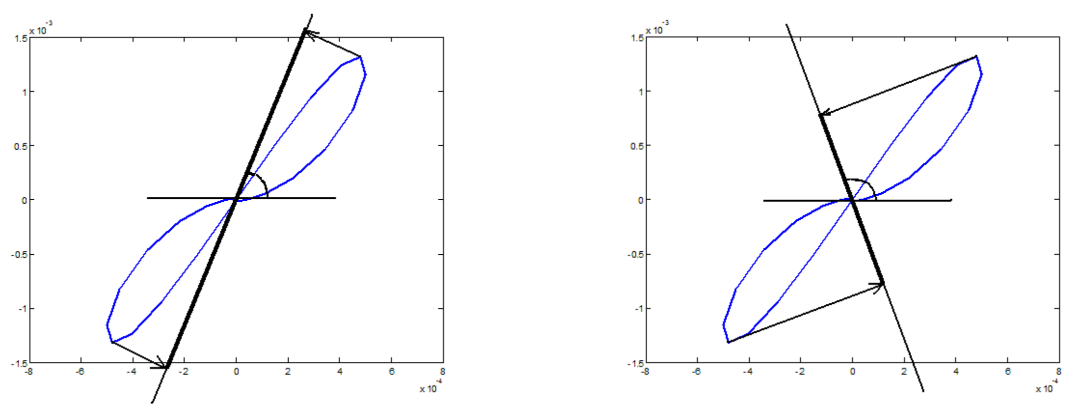

(a) (b)

Figure 3-6
Feature II with Different Angle α_1 and α_2

In Figure 3-7, Feature II at various defect depths and probe/coil offsets are plotted at $\alpha = 90^0$.

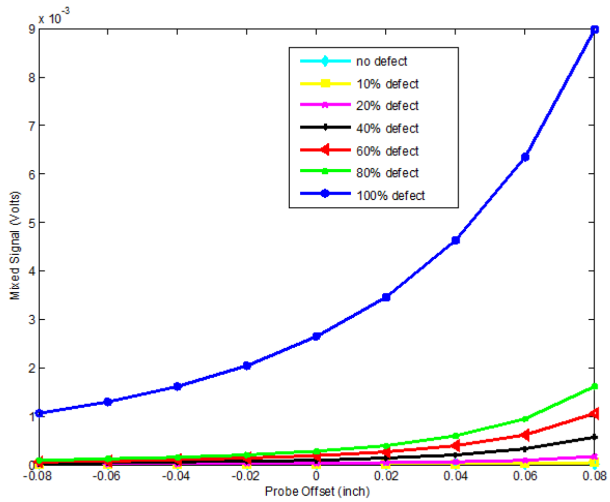

Figure 3-7
Projected Magnitude at α Equal to 90^0

The POD and the corresponding PFA curve for each angle α are calculated using a procedure similar to that used with Feature I. The Optimum Projection Angle (OPA) is determined by plotting the ratio POD/PFA versus various angle α as shown in Figure 3-8. From the peak value we conclude the OPA is equal to 108^0. Once the OPA is selected, the POD curves for various probe/coil offsets is estimated and plotted as seen in Figure 3-9.

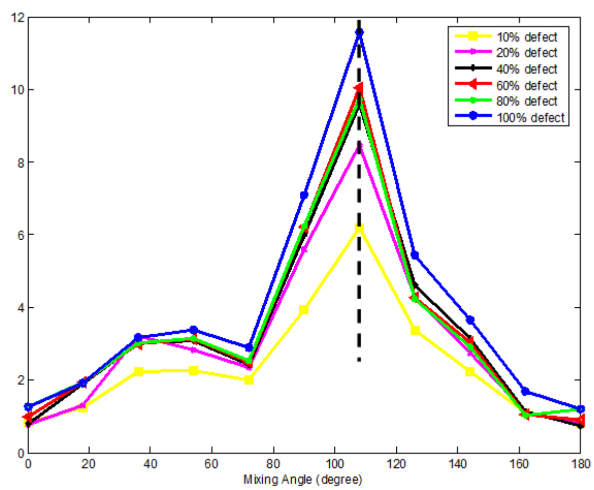

Figure 3-8
POD/PFA for Various α

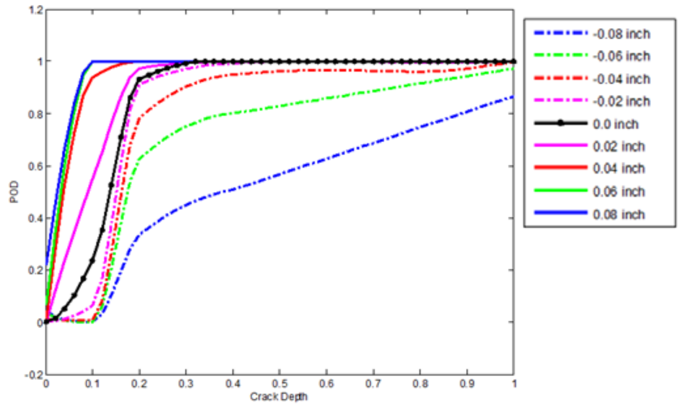

Figure 3-9
POD vs. Crack Size at OPA

3.2.2 Effectiveness of Features

The effectiveness of features I and II can be quantified in terms of the POD values. POD obtained with feature I (maximum signal magnitude) vs. POD using feature II (maximum projected signal magnitude) is plotted in Figure 3-10 which clearly demonstrates Feature II is more effective in detecting defects than Feature I.

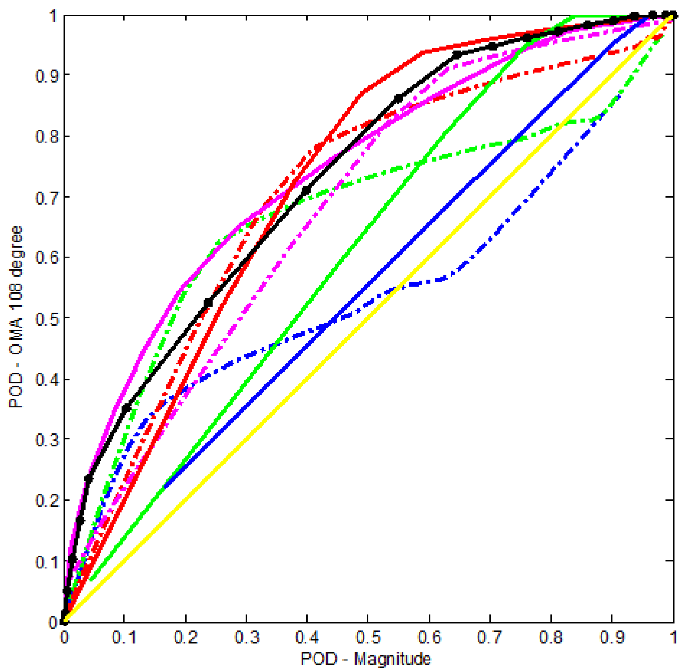

Figure 3-10
Comparison between POD from Feature I and Feature II

4

POD CALCULATION USING EXPERIMENTAL NOISE

4.1 Introduction

In this section we combine the simulation model generated signal together with measurement noise reported in the EPRI Report *Measuring and monitoring noise in steam generator tubing eddy-current data for tube integrity applications* [2], to estimate a POD curve for the procedure used in the ETSS # 27905.

This section explains how Model-based POD can be used to generate POD curves for any tube geometry, defect type, probe type, frequency in a fast and inexpensive manner.

The implementation procedure is summarized in the following steps:

1. The SGTSIM3D software is used to predict the signal from a selected probe, tube geometry defect geometry and location. Model predicted signals for different defect sizes are obtained by varying the defect depth during the simulation.
2. PDF (probability density function) from the measured noise obtained experimentally from the same tube geometry is numerically calculated.
3. A decision threshold corresponds to a 1% false call (PFA) is determined and the POD values corresponding to each defect is estimated.

The implementation of each step is presented in the following section. The POD results for flat wear volumetric defects are presented. A schematic of the methodology is shown in Figure 4-1.

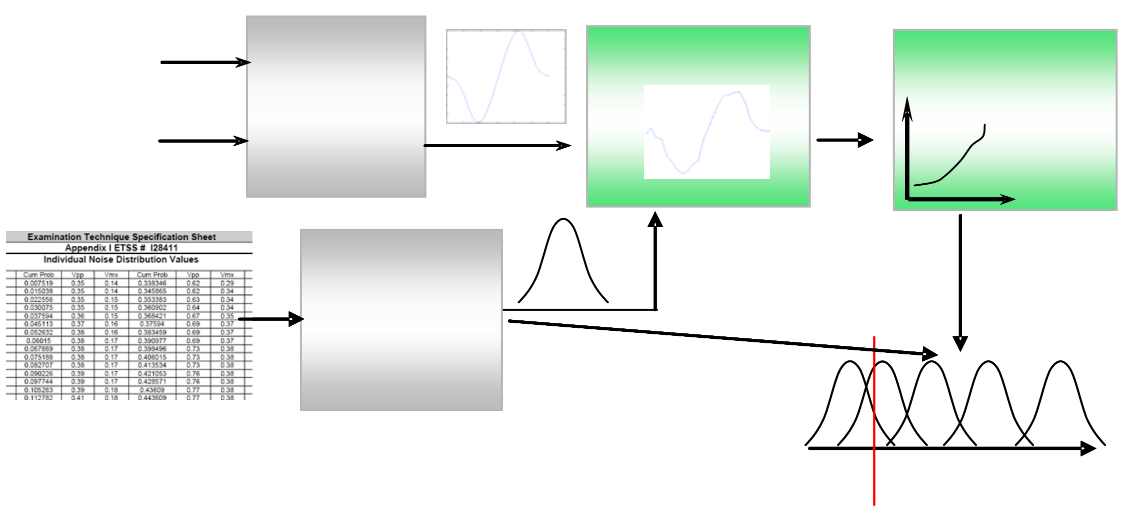

Figure 4-1
Application of MBPOD for Wear Flaws

4.2 Simulated Signals for Volumetric Wear Geometry

The simulation geometry for volumetric wears described in the ETSS sheet 27905 is shown in Figure 4-2. The geometry, probe, defect and operational parameters in the ETSS sheet were input to the simulation model to generate the noise free signals from a pancake coil probe at 300 kHz. The signal features Vpp and Vmax are used to generate POD curves.

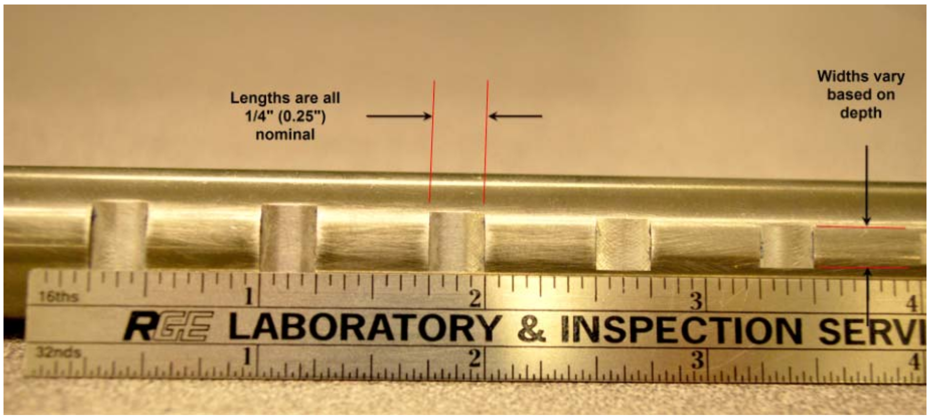

Figure 4-2
Simulation Geometry (ETSS Sheet 27905)

The simulated defect depth ranges from 0%, 30%, 45%, 60%, 75%, 90%, and 100%, which is the same as the ETSS sheet 27905. And the simulated signal is calibrated using the same standard as used in ETSS sheet. The comparison of signal feature values reported in ETSS sheet 27905 and that predicted by the simulation model is listed in Table 4-1. The signal matches very well, which validated the numerical model.

Table 4-1
The Comparison between ETSS and Simulation Signal for Pancake Probe with Feature of Vpp and Vmax

	Vpp		Vmax	
	ETSS (volts)	Simulation (volts)	ETSS (volts)	Simulation (volts)
100%	20	20	20	20
90%	18	18.4	11.7	13.4
75%	13.1	13.6	9.9	9.9
60%	7.9	8.3	6.9	6.89
45%	4.2	4.6	4.0	4.32
30%	2.2	3.2	2.2	2.73

The â vs. a curve, which is the signal feature vs. defect depth can therefore be obtained using the model and is plotted in Figure 4-3. The signal for an arbitrary defect depth from 0 to 100% can be estimated from these plots.

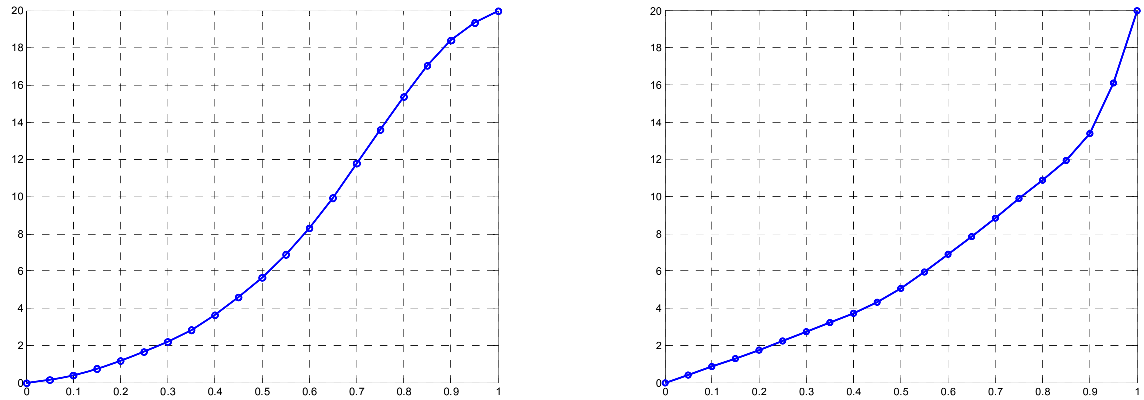

(a) (b)

Figure 4-3
Simulation Signal vs. Defect Depth for Pancake Probe with Feature of (a) Vpp (b) Vmax

4.3 Measurement Noise

The measurement noise data is extracted from the document of "Performance Demonstration Database – Appendix I ETSS # I28411". The original noise data is shown in Table 4-2 and the distribution of the noise is statistically analyzed in Figure 4-4. The noise distribution is not a normal distribution with zero mean as assumed in the logistic regression method (MAPOD) for POD calculation.

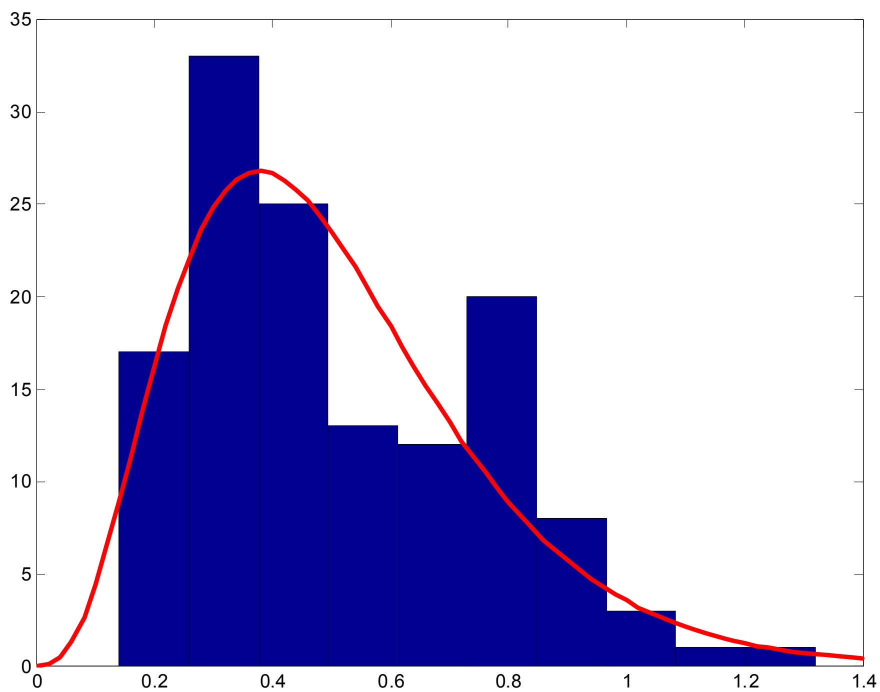

Figure 4-4
Statistical Distribution of the Measurement Noise in Table 4-2

Table 4-2
Data of Measurement Noise

Vpp	Vmx	Cum Prob	Vpp	Vmx	Cum Prob	Vpp	Vmx	Cum Prob
0.14	0.02	0.007519	0.35	0.14	0.338346	0.62	0.29	0.676692
0.15	0.02	0.015038	0.35	0.14	0.345865	0.62	0.34	0.684211
0.15	0.03	0.022556	0.35	0.15	0.353383	0.63	0.34	0.691729
0.15	0.04	0.030075	0.35	0.15	0.360902	0.64	0.34	0.699248
0.15	0.04	0.037594	0.36	0.15	0.368421	0.67	0.35	0.706767
0.15	0.04	0.045113	0.37	0.16	0.37594	0.69	0.37	0.714286
0.16	0.05	0.052632	0.38	0.16	0.383459	0.69	0.37	0.721805
0.17	0.06	0.06015	0.38	0.17	0.390977	0.69	0.37	0.729323
0.17	0.06	0.067669	0.38	0.17	0.398496	0.73	0.38	0.736842
0.19	0.06	0.075188	0.38	0.17	0.406015	0.73	0.38	0.744361
0.19	0.06	0.082707	0.38	0.17	0.413534	0.73	0.38	0.75188
0.19	0.06	0.090226	0.39	0.17	0.421053	0.76	0.38	0.759398
0.19	0.07	0.097744	0.39	0.17	0.428571	0.76	0.38	0.766917
0.2	0.07	0.105263	0.39	0.18	0.43609	0.77	0.38	0.774436
0.2	0.07	0.112782	0.41	0.18	0.443609	0.77	0.38	0.781955
0.25	0.07	0.120301	0.41	0.19	0.451128	0.77	0.38	0.789474
0.25	0.08	0.12782	0.41	0.19	0.458647	0.77	0.38	0.796992
0.26	0.08	0.135338	0.41	0.2	0.466165	0.77	0.4	0.804511
0.27	0.08	0.142857	0.41	0.2	0.473684	0.77	0.4	0.81203
0.27	0.09	0.150376	0.43	0.22	0.481203	0.77	0.4	0.819549
0.27	0.09	0.157895	0.43	0.22	0.488722	0.77	0.42	0.827068
0.28	0.09	0.165414	0.43	0.22	0.496241	0.77	0.42	0.834586
0.28	0.09	0.172932	0.43	0.22	0.503759	0.77	0.42	0.842105
0.29	0.09	0.180451	0.43	0.24	0.511278	0.77	0.43	0.849624
0.29	0.09	0.18797	0.43	0.24	0.518797	0.77	0.46	0.857143
0.29	0.09	0.195489	0.46	0.24	0.526316	0.78	0.46	0.864662
0.29	0.09	0.203008	0.46	0.24	0.533835	0.78	0.47	0.87218
0.29	0.09	0.210526	0.46	0.24	0.541353	0.78	0.47	0.879699
0.29	0.1	0.218045	0.48	0.24	0.548872	0.82	0.47	0.887218
0.29	0.1	0.225564	0.48	0.24	0.556391	0.82	0.48	0.894737
0.29	0.11	0.233083	0.48	0.25	0.56391	0.82	0.48	0.902256
0.29	0.11	0.240602	0.51	0.25	0.571429	0.85	0.5	0.909774
0.29	0.11	0.24812	0.51	0.25	0.578947	0.85	0.57	0.917293
0.29	0.11	0.255639	0.53	0.25	0.586466	0.86	0.61	0.924812
0.29	0.12	0.263158	0.53	0.25	0.593985	0.86	0.61	0.932331
0.3	0.12	0.270677	0.53	0.27	0.601504	0.87	0.62	0.93985
0.31	0.12	0.278195	0.53	0.27	0.609023	0.87	0.62	0.947368

4.4 POD Calculations for Volumetric Wear Geometry

The signal pdf's, generated by combining the simulation signal feature and measurement noise pdf, is shown in Figure 4-5. A decision threshold corresponding to 1% PFA is determined from the noise pdf and used in calculation of PODs of each defect and plotted in the POD curve in Figure 4-6.

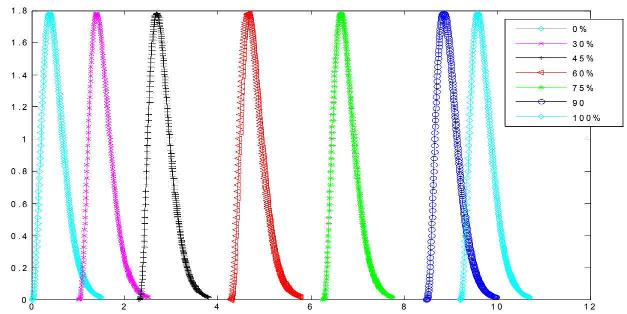

(a)

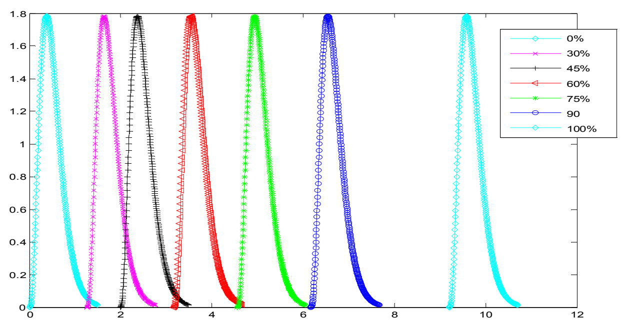

(b)

Figure 4-5
Signal PDF Distribution for Pancake Probe with Feature of (a) Vpp (b) Vmax

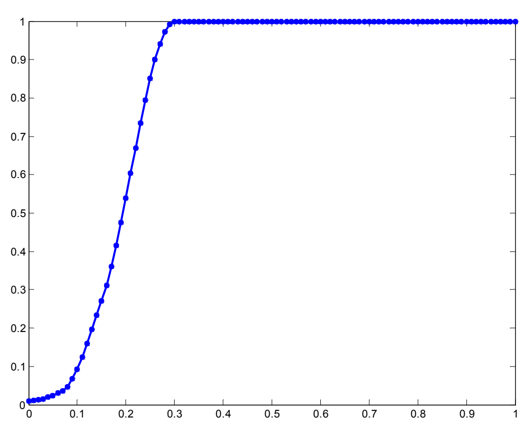

(a)

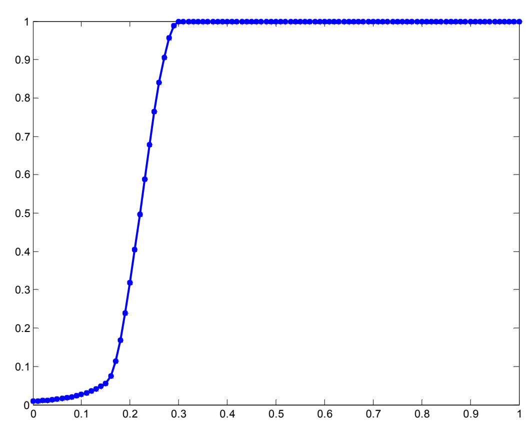

(b)

Figure 4-6
POD vs. Defect Depth for Pancake Probe with Feature of (a) Vpp (b) Vmax

4.4 Conclusion

This section shows how the proposed method can be used to produce POD curves for different defect and tube geometry in a fast and inexpensive way. The simulation model is implemented to generate the â vs. a curve. The noise distribution is statistically analyzed from the experimental noise data sheet. The approach yields accurate values of POD even when the noise is not zero mean or Gaussian.

The various tube/defect geometries and inspection condition can be simulated with the SGTSIM3D software, so that the POD curves for various tube geometries can be generated, such as freespan, tube support-center/edge, tube sheet, expansion transition-explosive/hardroll, AVB, sludge pile, loose part, U-Bend. Also the POD curves for various defect types can be easily generated, such as ID, OD, axial, circ, SCCs, dents, MBMs, wears, pits. Also, the POD curves with various probe types can be generated, such as bobbin, pancake, +pt, and array probes.

5
CONCLUSION AND FUTURE WORK

5.1 Conclusion

In this report, a model based approach for POD calculation for SG tube geometry is presented. The model-based approach is first applied to perform a sensitivity analysis of the POD with respect to different sources of variability in the eddy current SG inspection process. An initial set of parameters representing the sources of uncertainty was identified with input from EPRI. The concept was demonstrated using probe/coil offset parameter and its effect on the resultant POD. The approach can therefore be used to study the effect of single source of uncertainty on the resultant signal and thereby be used to optimize inspection setup and probe construction.

The POD was estimated using two different features (magnitude, projected signal magnitude). By comparing the results of the two POD curves, one can also determine the effectiveness of signal features for crack detection.

The model based approach was then used in combination with measured noise data available in the EPRI Tools project to generate POD curves for wear flaws. The simulation model is implemented to generate the â vs. a curve. The noise distribution is statistically analyzed from the experimental noise data sheet.

A variety of tube/defect geometries and inspection parameters can be simulated using the SGTSIM3D software, and the POD curves for various tube and flaw geometries can be generated, such as freespan, tube support-center/edge, tube sheet, expansion transition-explosive/hardroll, AVB, sludge pile, loose part, U-Bend and defect types such as ID, OD, axial, circ, SCCs, dents, MBMs, wears, pits. POD curves for various probe types such as bobbin, pancake, +pt, and array probes can also be generated.

5.2 Future Work

The proposed work has several potential applications as listed below.

5.2.1 Multi-variant POD algorithms

Generation of POD contours that combining two features simultaneously and extension to multiple features. This would have relevance to Auto analysis projects.

5.2.2 Sensitivity analysis for probe/system design by POD model

Effect of different sources of uncertainty on POD curves can be used in optimizing probe/system design and operation. An uncertainty factor with dramatic effect on POD can be identified as a "sensitive" factor in the probe/system design.

5.2.3 Transfer function

This approach uses empirical data and numerical models to transfer POD measured on EDM notches to real cracks thereby providing a process by which POD curves for natural defects in complex geometries can be generated.

The transfer function steps are as follows:

1. Generate artificial flaws in geometry of interest
2. Generate artificial flaws in flat plate
3. Generate cracks in flat plate
4. Establish relationship between cracks and EDM notches for flat plate using well-controlled lab studies
5. Determine variability through POD study of EDM notches in geometry of interest
6. Utilize relationship from flat plates (step 4) and variability data from notches (step 5) to generate variability data for cracks in geometry of interest
7. Generate POD vs. crack size curves for the geometry of interest

6
REFERENCES

1. *Updates on the Tools for Integrity Assessment Project*. EPRI, Palo Alto, CA: 2007 1014756.
2. *Measuring and Monitoring Noise in Steam Generator Tubing Eddy-Current Data for Tube Integrity Applications*. EPRI, Palo Alto, CA: 2008 1016554
3. *Tools for Integrity Assessment Project Technical Report*. EPRI, Palo Alto, CA: 2006 1014567.
4. C. Annis and J. Knopp, "Comparing the Effectiveness of $a_{90/95}$ Calculations", *Review of Progress in QNDE*, Vol. 26, 2006, pp. 1767-1774.
5. Z. Zeng, "Application of POD Studies and Robust Design to Electromagnetic NDE", Ph.D. Dissertation, 2002.

A TRANSLATED TABLE OF CONTENTS

DISCLAIMER OF WARRANTIES AND LIMITATION OF LIABILITIES

ORGANIZATION(S) THAT PREPARED THIS DOCUMENT

Electric Power Research Institute (EPRI)

蒸気発生器の管理プログラム:モデルを使用したエディ電流 SG 検査指標の検知確率

1020630

技術アップデート、2010 年 3 月

製品説明

経年劣化した航空機、発電所、およびガス輸送用パイプラインの検査では、検査システムが検査要件を実際に満たしているかどうかを確認することが重要です。これらの適用では、重大なきずを検出するための検査システムの性能は、その検知確率(POD)および観測された信頼限界の点から定量化されます。異なる非破壊検査技術および検査官によるばらつきという限界が、誤拒否および誤受け入れエラーを頻繁に引き起こします。さらに、リフトオフ、プローブ揺れ(オフセット)、コイル傾斜、材料特性、およびきず方向などの運用パラメータにおける不確実性が、同じきずの公称寸法に対する信号強度で広がることになります。検査パラメータにおけるこれらの変数および不確実性によって引き起こされる信号拡散についての定量的知識は、事業者が決定戦略を合理化する手助けとなります。適正な信頼限界による POD の推定には、相当量の実験データが必要とされます。実験データはほとんど理想的な条件の下で収集されます。このため、頻繁に、POD の誤推定を引き起こすことになります。

このプロジェクトでは、ユーザインターフェイスを持つ別のプロジェクトによって開発されたシミュレーションモデルが、データベースを作成し、重大な場所での重大なきずの POD を計算するための体系的なモデルに基づく研究を実施するために、使用されます。実験パラメータの不確実性の定量的知識は、POD 曲線を生成する数値モデルと併用して使用されます。POD モデルに基づく定量的評価は、
適切な条件の下で検査システムの性能を正確に評価する場合にも使用できます。

結果と研究成果

この報告書には、蒸気発生器(SG)管形状の POD 計算のためのモデルに基づく方法が提示されています。この方法は、エディ電流 SG 検査プロセスにおいて、さまざまな変動原因ごとに POD の感度解析を実行するために最初に適用されます。不確実性の原因を示す初期のパラメータセットは、電力研究所(EPRI)からの入力に従って分類されました。この概念は、プローブ/コイルのオフセットパラメータおよびこれに伴う POD への影響を使って実証されました。この方法は、不確実性の単一の原因の、これに伴う信号への影響を研究し、その後検査設定とプローブ構成を最適化するために使用されます。

課題と目的

きずの種類(内径(ID)、外径(OD)、軸方向、円周、応力腐食割れ(SCC)、へこみ、製造時のバフマーク(MBM)、磨耗、および穴など)に加えて、管およびきずの形状(フリースパン、管支柱の中心/端、管シート、継手移動の爆発/ハードロール、振れ止め金具(AVB)、スラッジパイル、緩んだパーツ、および U 字屈曲など)に関して、SGTSIM3D ソフトウェアおよび POD 曲線を使ってシミュレーションされる各種の管/きずの形状および検査パラメータが、作成されます。プローブタイプ(ボビン、パンケーキ、+ポイント、および配列プローブなど)ごとの POD 曲線も生成されます。

応用、値、および使用

POD 曲線上の不確実性のさまざまな原因の影響が、プローブ/システムの設計および運用を最適化する際に使用されます。POD に劇的影響を与える不確実性要因は、プローブ/システムの設計における「感度」係数として特定されます。

EPRI の観点

検査プロセスの基礎的物理学を記述する数学的(積分または微分)方程式に解決策を提供する物理学ベースの計算モデルは、POD 曲線の生成において重要な役割を果たします。これらのモデルは、検査部品における界分布および電流分布の可視化を可能にします。これにより検査パラメータを最適化することができ、検査手順の信頼性を高めます。モデルは、不確実性の信号強度への影響を研究し傾向を示すための方法として、いくつかの業界で使用されてきました。数値計算を使って信号振幅の統計的分布が作成されると、POD および誤判定は、受け入れ範囲内の信号分布を統合することによって推定することができます。

方法

研究者たちは、ノイズ分布などの現場からのデータとともに、計算モデルを使用して、コンピュータモデリングによる実験データを複製します。結果は実験による方法に比べてはるかに少ない時間、はるかに少ない費用で得られます。

キーワード
検知確率
モデリング
蒸気発生器

目次

図リスト

表リスト

증기 발생기 관리 프로그램: 모델을 활용한 와전류 (Eddy Current) SG 검출 확률 점검시 지침사항

1020630

기술 업데이트, 2010 년 3 월

제품 설명

노후한 항공기, 발전소, 가스 공급 파이프라인 등을 점검할 때는, 점검 시스템이 실제로 점검 요건을 충족하는지 확인하는 것이 중요합니다. 이러한 용도에서는, 결정적인 결함을 검출하는 점검 시스템의 능력을 그 검출확률(POD) 및 관찰된 확실성 한도 (observed confidence bounds)를 따져서 수치화합니다. 여러 가지 비파괴 기법과 점검인력의 변동성으로 인한 한계 때문에 잘못된 거부와 잘못된 합격판정의 오류가 일어날 경우가 자주 있습니다. 더욱이, 리프트-오프, 검출장치(probe)의 불안정 (오프셋), 코일 경사, 자재 특성, 결함의 방향 같은 조작 파라미터 (operational parameter)의 불확실성은 명목상 결함의 크기가 동일한 경우에도 신호 강도의 분산을 일으킵니다. 이러한 변수들과 점검 파라미터의 불확실성 때문에 발생된 신호 분산을 수량적으로 파악해 두면 운용자들이 합리적인 결정 방침을 세우는 데 도움이 됩니다. 양호한 확실성 한도를 이용해 POD 를 산출하려면 상당량의 실험 데이터가 필요합니다. 실험 데이터는, 이상적 조건에 근접한 조건에서 수집할 경우가 매우 자주 있으므로, 그 때문에 POD 가 잘못 산출될 수 있습니다.

이 프로젝트에서는, 별도의 프로젝트를 통해 개발된 사용자 인터페이스가 있는 시뮬레이션 모델을 사용해 데이터베이스를 생성하고 중요한 위치에서의 중대한 결함에 대한 POD 를 산출하는 체계적인 모델 기반의 연구를 수행합니다. 실험 파라미터의 불확실성을 수치로 파악해 두면 수치 모델과 함께 POD 곡선을 작성하는 데 이용할 수 있습니다. 그런 다음 POD 모델에 근거한 수량적 분석 결과를 적정 조건하에서 점검 시스템의 성능을 정확하게 평가하는 데 이용할 수 있습니다.

결과와 발견된 사실

이 보고서에서는, 증기 발생기 (SG) 튜브의 입체구조에 대한 POD 산출을 위한 모델 기반의 접근법을 설명합니다. 이 접근법은 와전류 SG 점검 과정에서 변동성의 여러 가지 원인을 대상으로 POD 에 대한 감도 분석을 실시하는 데 우선 적용합니다. EPRI(전력산업 연구소)에서 제공한 정보를 이용해 불확실성의 원인을 표현하는 파라미터들의 초기 집합을 확인하였습니다. 이 개념은 검출장치/코일 오프셋 파라미터와 그것의 결과로 얻어진 POD 에 대한 그 영향을 이용하여 설명되었습니다. 그러므로 이

접근방식은 단일한 불확실성의 원인이 결과로 생성된 신호에 미칠 영향을 연구하고, 다음으로 점검방식을 설정하고 검출장치 구성을 최적화하는 데 이용할 수 있습니다.

문제점과 목표

SGTSIM3D 소프트웨어를 사용해 여러 가지 튜브/결함 입체구조와 점검 파라미터들을 시뮬레이션할 수 있으며, 프리스팬(freespan), 튜브 지지물 중심/가장자리, 튜브시트, 팽창전이 폭발물(expansion transition-explosive)/하드롤(hardroll), 항진동막대(anti-vibration bar: AVB), 슬러지 퇴적물 (sludge pile), 느슨해진 부품 및 U 형곡관(U-bend) 같은 여러 가지 튜브와 결함의 입체구조에 대한 POD 곡선은 물론, 내경(ID), 외경(OD), 축방향(axial), 원주형(circumferential), 응력부식균열(SCC), 눌린 자국, 제조시 충격 흔적(MBM), 마손, 및 구멍(pit) 같은 결함 유형들을 생성할 수 있습니다. 여러 종류의 검출장치 — 보빈, 팬케이크, +pt, 및 어레이 검출장치 (array probe) 등 — 에 대한 POD 곡선들도 생성 가능합니다.

용도, 가치 및 사용

여러 가지 불확실성의 원인들이 POD 곡선에 미치는 영향을 검출장치/시스템 설계 및 작동을 최적화하는 데 이용할 수 있습니다. 검출장치/시스템을 설계할 때, POD 에 극적인 영향을 미치는 불확실성 인자를 " 고감도(sensitive)" 인자로서 특정할 수 있습니다.

EPRI 의 입장

점검 과정의 기초가 되는 물리학을 설명하는 수학식 (적분 또는 미분)에 해답을 제공하는 물리학에 근거한 계산 모델은 POD 곡선을 작성하는 데 중요한 역할을 할 수 있습니다. 이러한 모델들은 점검 부위에서 필드와 현재의 분포상태를 시각적으로 표시할 수 있게 해 주고, 이것은 다시 점검 파라미터를 최적화하고 점검 과정의 신뢰도를 개선하는 데 도움이 됩니다. 몇몇 업종에서 신호 강도에 미치는 불확실성의 영향을 연구하고 경향을 파악하는 방법으로서 모델을 사용하였습니다. 수치 계산을 이용해 신호 진폭 (signal amplitude)의 통계적 분포를 확정한 후에, 합격범위(acceptance range) 내의 신호 분포를 적분하여 POD 와 허위요청(false call)을 추산할 수 있습니다.

접근방식

연구자들은 컴퓨터 모델을 사용해 실험 데이터를 재현하고자, 노이즈 분포와 같은 필드에서 얻은 데이터와 함께 계산용 모델을 사용하였습니다. 결과는 실험적 접근방식에 비해 훨씬 짧은 시간과 비용만으로 얻어집니다.

주요 어휘

검출 확률

모델 작성

증기 발생기

목차

그림 목록

표 목록

Programa de Gestión de Generadores de Vapor: Probabilidad de detección basada en modelos de las indicaciones de inspección de generadores de vapor por corrientes inducidas

1020630

Actualización técnica, marzo de 2010

DESCRIPCIÓN DEL PRODUCTO

En la inspección de las tuberías de transmisión de gas, centrales eléctricas y aviones antiguos, es importante determinar si el sistema de inspección realmente cumple los requisitos de inspección. En estas aplicaciones, la capacidad de un sistema de inspección para detectar defectos importantes se contabiliza en términos de su probabilidad de detección (probability of detection, POD) y en los umbrales de confianza observados. Las limitaciones de las diferentes técnicas de inspección no destructiva y la variabilidad de inspectores a menudo producen rechazos erróneos y falsos errores de aceptación. Además, las incertidumbres en los parámetros operativos, tales como la orientación de errores, las propiedades de los materiales, la oscilación de bobinas, la oscilación (desajuste) de sondas y la elevación conducen a una difusión de la fuerza de la señal para el mismo tamaño de defecto nominal. El conocimiento cuantitativo de la difusión de la señal causado por estas variables e incertidumbres en los parámetros de inspección puede ayudar a los operadores a racionalizar sus estrategias de decisión. La estimación de la probabilidad de detección con un buen umbral de confianza requiere una cantidad importante de datos experimentales. En muchas ocasiones, los datos experimentales se recopilan en condiciones casi idealizadas, por lo que es posible que se produzcan cálculos erróneos de la probabilidad de detección.

En este proyecto, el modelo de simulación desarrollado a través de otro proyecto con una interfaz de usuario se ha utilizado para generar una base de datos y dirigir un estudio basado en un modelo sistemático para calcular la probabilidad de detección de defectos graves en ubicaciones críticas. Se puede utilizar el conocimiento cuantitativo de las incertidumbres en los parámetros experimentales junto con los modelos numéricos a fin de generar curvas de probabilidad de detección. Asimismo, se pueden utilizar las evaluaciones cuantitativas basadas en modelos de probabilidad de detección para evaluar con precisión el rendimiento de un sistema de inspección bajo las condiciones adecuadas.

Resultados y conclusiones

En este informe se presenta un enfoque basado en modelos sobre los cálculos de probabilidad de detección para la geometría de los tubos de los generadores de vapor. En primer lugar, este enfoque se aplica para llevar a cabo un análisis de sensibilidad de la probabilidad de detección con respecto a las diferentes fuentes de variabilidad en el proceso de inspección de generadores de vapor por corrientes inducidas. Con ayuda de información procedente del Electric Power Research Institute (EPRI), se ha identificado un conjunto inicial de parámetros que representan las fuentes de incertidumbre. El concepto se demostró mediante un parámetro de desajuste de sonda/bobina y su efecto en la probabilidad de detección resultante. También se puede utilizar este enfoque para estudiar el efecto de una fuente individual de incertidumbre en la señal resultante y, posteriormente, para optimizar la configuración de las inspecciones y la construcción de sondas.

Desafíos y objetivos

Se puede simular una variedad de parámetros de inspección y geometrías de defectos/tubos mediante el software SGTSIM3D y las curvas de probabilidad de detección para diferentes geometrías de defectos y tubos, tales como huecos, borde/centro de soporte de tubos, placa tubular, transición de expansión (explosiva/rodamiento), barra antivibración (AVB), pila de sedimentos, pieza suelta y curva en U, además de tipos de defectos tales como, grietas por corrosión debido a la tensión tanto circunferenciales, axiales, como de diámetro interior (DI) y de diámetro exterior (DE), abolladuras, marcas de fabricación, desgaste y picaduras. Se pueden generar curvas de probabilidad de detección para diferentes tipos de sondas como, por ejemplo, sondas matriz, +pt, pancake y de bobina.

Aplicaciones, valor y uso

El efecto de las diferentes fuentes de incertidumbre en curvas de probabilidad de detección se puede utilizar para optimizar el funcionamiento y el diseño de los sistemas y sondas. Un factor de incertidumbre con un efecto drástico en la probabilidad de detección se puede identificar como factor "sensible" en el diseño de los sistemas/sondas.

La perspectiva de EPRI

Los modelos computacionales que ofrecen la solución a las ecuaciones matemáticas (integrales o diferenciales) y que describen la física subyacente de un proceso de inspección pueden desarrollar un papel importante en la generación de curvas de probabilidad de detección. Estos modelos permiten la visualización de las distribuciones de corriente y de campo en las partes inspeccionadas, lo que a su vez contribuye a optimizar los parámetros de inspección y a fortalecer la fiabilidad de los procedimientos de inspección. Los modelos se han utilizado en varias industrias como método para estudiar y modificar los efectos de las incertidumbres de la fuerza de la señal. Una vez que la distribución estadística de la amplitud de la señal se ha establecido usando cálculos numéricos, la probabilidad de detección y los falsos positivos se pueden calcular mediante la integración de la distribución de la señal dentro de los límites de aceptación.

Enfoque

Los investigadores utilizaron modelación computacional junto con datos recopilados en el campo como, por ejemplo, las distribuciones del ruido, para reproducir los datos experimentales a través de la modulación computacional. Los resultados se han obtenido en un tiempo menor y con un coste inferior en comparación con los enfoques experimentales.

Palabras clave

Probabilidad de detección
Modelación
Generador de vapor

CONTENIDO

LISTA DE FIGURAS

LISTA DE TABLAS

Export Control Restrictions

Access to and use of EPRI Intellectual Property is granted with the specific understanding and requirement that responsibility for ensuring full compliance with all applicable U.S. and foreign export laws and regulations is being undertaken by you and your company. This includes an obligation to ensure that any individual receiving access hereunder who is not a U.S. citizen or permanent U.S. resident is permitted access under applicable U.S. and foreign export laws and regulations. In the event you are uncertain whether you or your company may lawfully obtain access to this EPRI Intellectual Property, you acknowledge that it is your obligation to consult with your company's legal counsel to determine whether this access is lawful. Although EPRI may make available on a case-by-case basis an informal assessment of the applicable U.S. export classification for specific EPRI Intellectual Property, you and your company acknowledge that this assessment is solely for informational purposes and not for reliance purposes. You and your company acknowledge that it is still the obligation of you and your company to make your own assessment of the applicable U.S. export classification and ensure compliance accordingly. You and your company understand and acknowledge your obligations to make a prompt report to EPRI and the appropriate authorities regarding any access to or use of EPRI Intellectual Property hereunder that may be in violation of applicable U.S. or foreign export laws or regulations.

The Electric Power Research Institute Inc., (EPRI, www.epri.com) conducts research and development relating to the generation, delivery and use of electricity for the benefit of the public. An independent, nonprofit organization, EPRI brings together its scientists and engineers as well as experts from academia and industry to help address challenges in electricity, including reliability, efficiency, health, safety and the environment. EPRI also provides technology, policy and economic analyses to drive long-range research and development planning, and supports research in emerging technologies. EPRI's members represent more than 90 percent of the electricity generated and delivered in the United States, and international participation extends to 40 countries. EPRI's principal offices and laboratories are located in Palo Alto, Calif.; Charlotte, N.C.; Knoxville, Tenn.; and Lenox, Mass.

Together...Shaping the Future of Electricity

Programs:

Nuclear Power

Steam Generator Management Program

1020630

Electric Power Research Institute
3420 Hillview Avenue, Palo Alto, California 94304-1338 • PO Box 10412, Palo Alto, California 94303-0813 USA
800.313.3774 • 650.855.2121 • askepri@epri.com • www.epri.com